COARSE AND TURBO SYNCHRONIZATION: A CASE-STUDY FOR DVB–RCS

Susanne Godtmann, Niels Hadaschik, Wolfgang Steinert, André Pollok, Gerd Ascheid, and Heinrich Meyr

Institute for Integrated Signal Processing Systems, RWTH Aachen University
Templergraben 55, 52056 Aachen, Germany
www.iss.rwth-aachen.de

ABSTRACT

In this paper, we examine turbo synchronization in the presence of carrier frequency uncertainties and phase offsets for the DVB–RCS standard. As turbo synchronization can only achieve high estimation accuracy if the initial parameter offset is sufficiently small, we employ a coarse synchronization unit for pre-compensation. Especially for frequency offset estimation, the position of known pilot symbols within the burst is of significant importance. Therefore, we optimize both their distribution and their amount in order to guarantee reliable synchronization, high bandwidth efficiency, high power efficiency and excellent BER performance.

1. INTRODUCTION

With DVB–RCS [1], a standard has been introduced whose implementation is very challenging due to transmission at low SNR coupled with short burst lengths. Accurate synchronization under these circumstances is of significant importance [2].

The Digital Video Broadcasting (DVB) project, a consortium of more than 200 public and private sector organizations in the television industry, was founded by ETSI in 1993. With DVB-S, a packet-based broadcast system has been introduced that distributes the signal via geostationary satellites. Although video broadcasting only requires a downlink, the provision of an additional uplink is a necessity to enable internet applications and interactive television as they involve user data requests. DVB-S was therefore extended by an interaction channel, known as DVB Return Channel via Satellite (DVB–RCS). As DVB–RCS is independent of wiring, it is attractive for even the most remote areas. With uplink data rates of up to 2 Mbps it can be considered as competitive alternative to DSL techniques.

As the satellite terminals are supposed to be both low-cost and low-power consuming, synchronization of the uplink satellite channel is quite a challenge. Even though DVB–RCS is not designed for high velocities, a mobile application without steady power supply is desirable. Thus, transmit energy should be as low as possible demanding for a strong channel code. DVB–RCS foresees a parallel concatenated turbo code, which is iteratively decoded at receiver side. The iterative processing at receiver side and the high sensitivity of turbo codes against synchronization errors, immediately implies the use of turbo synchronization.

Turbo synchronization has recently yield very promising results, [3] and [4] are just two of various publications. It has been demonstrated in the literature that in case of convergence, turbo synchronization offers equally precise estimates as purely data-aided (DA) estimators; with the advantageous difference that turbo synchronization does not require pilot symbols. Thus, an estimate produced by a turbo synchronization unit is equivalently precise to an estimate that would be produced by a DA estimator, if the whole data burst consisted only of pilot symbols.

However, "in case of convergence" is a key issue for turbo synchronization. The estimation range is narrow, especially for frequency offset estimation. This problem may be resolved by hypothesis testing as it has been proposed for phase offset estimation in [5]. However, in a realistic system with frequency inaccuracies, this results in unacceptably high receiver complexity and, therefore, high latency. Thus, data-aided coarse synchronization is inevitable in order to initialize turbo synchronization reliably and to trigger its convergence.

In this paper, we consider the whole system approach incorporating coarse synchronization, turbo synchronization, and decoding. We pay special attention to an optimized positioning of pilot symbols within the burst structure, so that an accurate coarse synchronization is assured. It is shown that the coarse synchronization is precise enough to enable the convergence of the subsequent turbo synchronization, but that no bandwidth is wasted on pilot symbols providing an accuracy, which is achievable by the turbo synchronization unit at the only cost of a slightly higher receiver complexity.

The paper is structured as follows: Section 2 introduces the considered transmission model. Section 3 shortly summarizes the fundamental points of the DVB–RCS standard. The issue of the pilot constellation is addressed in Section 4. Section 5 and Section 6 deal with the coarse and the turbo synchronization, respectively. Simulation results are presented in Section 7 and Section 8 concludes this work.

2. TRANSMISSION MODEL

The transmission model considered in this paper is shown in Fig. 1. Information bits are grouped into packets, encoded and mapped onto a modulation alphabet $\mathcal{A}$. The resulting K_d data symbols are then transmitted over an additive white Gaussian noise (AWGN) channel together with K_p pilot symbols. The total number of symbols per burst is denoted as $K = K_d + K_p$.

As the DVB-RCS standard defines rather strict constraints on symbol timing, perfect timing synchronization can be considered a realistic assumption. The received baseband signal after matched filtering and sampling can then be modelled as

$$r_k = a_k \cdot e^{j(2\pi \Delta f T k + \vartheta)} + n_k, \tag{1}$$

with T being the symbol duration. The transmitted and the received symbol at sampling instant k are denoted as a_k and r_k, respectively. We denote the unmodulated symbol as $z_k = r_k a_k^*$, where a_k^* represents the complex conjugate of a_k. Unit energy symbols are assumed, i.e. $E_s = E\{|a_k|^2\} = 1$. Furthermore, n_k are the samples of complex-valued AWGN with independent real and imaginary parts, each having zero-mean and variance $N_0/(2E_s)$.

A. Pollok is with the Institute for Telecommunications Research, University of South Australia. W. Steinert is with AUDENS Telecommunications Consulting GmbH.

This work has been financed by BMBF, the German Federal Ministry of Education and Research and supported by DLR, the German Aerospace Center. Special thanks go to Dr. M. Keller. S. Godtmann thanks the Deutsche Telekom Stiftung for its financial support.

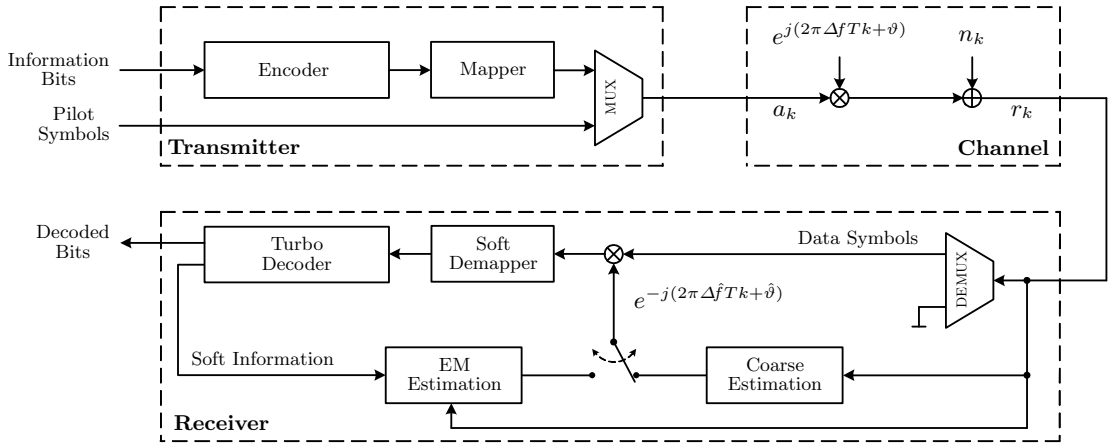

Figure 1: System Model

In addition to the noise component, a phase offset ϑ and a frequency offset Δf are introduced by the physical channel and the oscillators. As the DVB–RCS standard employs short bursts, phase and frequency offset can be assumed to be constant for the duration of one burst.

Let the time scale of each burst be defined such that the center symbol corresponds to $k = 0$. Furthermore, let $\mathcal{K}$ denote the entire set of time instants. The subsets $\mathcal{K}_d$ and $\mathcal{K}_p$ are related to data and pilot symbols. For later use, we define the K-dimensional vectors $\boldsymbol{r}$ and $\boldsymbol{a}$ as the concatenation of the symbols r_k and a_k, respectively.

3. DVB–RCS PARAMETERS

In this paper, we focus on traffic burst transmission in DVB–RCS. The two existing formats are ATM and MPEG2, consisting of 424 and 1504 information bits, respectively. The interleaver size is fixed – i.e. that adding pilot symbols prolongs the burst. As DVB–RCS makes use of frequency hopping, bursts are generally neither transmitted in consecutive time-slots nor at the same frequency. Thus, receiver synchronization needs to be performed burst by burst. Due to space limitations phase noise is not considered in this paper. As timing synchronization is very accurate due to the constraints given in the standard, we here consider frequency offset and phase offset estimation.

Since DVB–RCS terminals are supposed to be rather low-cost, the frequency offset can be significant. An offset of up to 20kHz may occur. Depending on the symbol rate, this may result in normalized offsets ΔfT, that cannot be handled by the receive filter. Therefore, here, we limit the maximum frequency offset to $\Delta fT = 0.08$. In case larger offsets occur, one has to deal with a pre-compensation before matched filtering at the receiver.

The modulation as foreseen in [1] is Gray-mapped QPSK. The code rates range from $r = 1/3$ to $r = 6/7$.

4. PILOT SCHEMES

Since DVB–RCS transmission takes place at very low SNR, pilot symbols for data-aided coarse synchronization are needed. For bandwidth efficiency, it is desirable to keep the ratio $\eta = K_p/K$ of pilot symbols as low as possible. However, accurate synchronization is only feasible, if the total amount of energy within the pilot symbols $K_p \cdot E_s/N_0$ is above the SNR threshold of a realistic DA estimator. Hence, short bursts usually require a higher η than large bursts.

DVB–RCS foresees a pure preamble of variable length [1]. However, a preamble constellation is suboptimal, especially for frequency synchronization. The theoretically optimal constellation is splitting the pilot sequence into two parts and placing one part as pure postamble at the end of the burst [6]. The theoretical estimation gain compared to the pure preamble constellation is significant, e.g. for a burst consisting of 1000 data symbols and 100 pilot symbols it is 31dB. Due to this reason, we refrain from using the preamble constellation and consider the pre/postamble (PP) structure (see Fig. 2(a)). However, it should be stressed, that if the amount of pilot symbols is raised significantly, synchronization is, of course, also possible for a preamble constellation.

At low SNR, the pre/postamble constellation exhibits a significant drawback: realistic estimators have difficulties in achieving the theoretical optimum in terms of estimation accuracy.

The reason is intuitive: DA frequency estimators have a limited estimation range, meaning that the phase increment between adjacent pilot symbols must not exceed π. In case of a pre/postamble constellation, the phase increments within the preamble and within the postamble are manageable with common estimators (as $|\Delta fT| < 0.08$). However, in order to profit from the large mean distance between pre- and postamble (denoted as D), a hierarchical estimation process is inevitable. This means that the first estimation step, solely based on pre- and postamble separately, must reduce the frequency offset such that $D \cdot |\Delta fT| < 0.5$. Depending on the accuracy of the first estimation stage and on the distance D, this condition is hard to be met.

In order to circumvent this problem, we introduce a spacing L into both, pre- and postamble (Fig. 2(b)). This has a positive effect on the estimation accuracy of the initial estimation stage – it is straightforward to show, that the theoretical achievable mean square estimation error (MSE) is then anti-proportional to L^2. Furthermore, the spacing L decreases the distance D. These two effects considerably help to meet the condition $D \cdot |\Delta fT| < 0.5$. The inherent spacing in the pre/postamble depends on the burst length

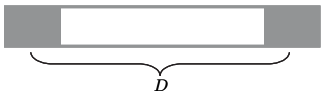

(a) Pre-/Postamble (PP)

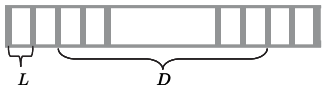

(b) L-spaced Pre-/Postamble (L-PP)

(c) Preamble - Midamble - Postamble (P-M-P)

Figure 2: Pilot schemes.

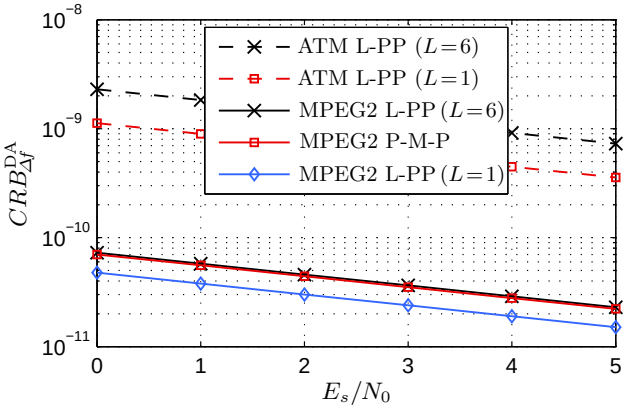

Figure 3: CRB for DA frequency estimation.

and the maximum frequency offset that may occur. Assuming a maximum frequency offset of $|\Delta f T|=0.08$, the spacing is limited to $L\leq 6$ in order to assure $L\cdot|\Delta f T|<0.5$.

In the Appendix, we analytically illustrate the above-mentioned condition and we demonstrate for the example on the ATM burst that $\eta>0.11$ has to be met in order to guarantee reliable coarse frequency synchronization for $r=1/3$. Applying the results given in the appendix to the MPEG2 burst yields the condition $\eta>0.083$ for $L=6$ and code rate $r=1/3$.

An alternative pilot symbol constellation suitable for long bursts is a pre/postamble structure with $L=1$, where additional pilot symbols are multiplexed into the data symbols as midamble. An additional advantage of this constellation is that it is possible to track phase noise. This constellation is denoted as P-M-P (Fig. 2(c)). Using the same approach as illustrated in the appendix, one can show that for long bursts the P-M-P constellation theoretically allows for a smaller η than the L-PP constellation ($\eta>0.05$ for an MPEG2 burst coded with $r=1/3$) while achieving approximately the same performance.

The so-called Cramér-Rao Bound (CRB) establishes a lower bound for the mean square estimation error (MSEE) that an estimator can achieve under certain conditions. Fig. 3 illustrates the effects of different pilot constellations on the data-aided CRB ($CRB_{\Delta f}^{\mathrm{DA}}$) for the considered traffic frames coded at $r=1/3$. The ratio of pilot symbols is chosen to $\eta=0.13$ for the ATM frame and to $\eta=0.08$ for the MPEG2 burst. The P-M-P pilot constellation is dimensioned such that pre- and postamble consist of $K_p/4$ each. The residual $K_p/2$ pilot symbols are distributed equally between pre- and postamble. It can be seen, that for the MPEG2 burst and $\eta=0.08$ the $CRB_{\Delta f}^{\mathrm{DA}}$ for the L-PP constellation and the P-M-P constellation almost coincide.

5. COARSE SYNCHRONIZATION

The coarse synchronization unit consists of a frequency and a phase estimator. Frequency synchronization is performed prior to phase offset estimation. In order to keep the receiver complexity acceptable, the frequency estimator is purely data-aided.

In the case of an L-PP pilot constellation, the whole coarse synchronization chain is subdivided into three subsequent steps. Each step consists of an estimation followed by a correction, where the estimation is of increasing accuracy, but covers a smaller frequency range. The first stage makes use of a simple Fast-Fourier-Transform in order to reduce the frequency offset to a value treatable with a more accurate estimator [7]. After pre-correcting the received signal with the initial estimate from the first stage, the L&R estimator is applied [8]. This algorithms delivers a more accurate estimate and performs close to the theoretical limit. Its main drawback - the limited estimation range - is circumvented by the first estimation stage.

As the pilot constellation is not equally spaced, pre- and postamble are treated separately by the first two synchronization stages. The estimates of pre- and postamble are then linearly combined and subsequently used for correction. It is the task of the third estimation stage to profit from the mean distance D between pre- and postamble and to finally perform close to the theoretical limit taking into account the overall pilot constellation. This estimator considers the averaged phase increment between pre- and postamble [2]

$$\Delta\hat{f}T=\frac{1}{2\pi D}\arg\left\{\left(\sum_{k\in\mathcal{K}_{\mathrm{pre}}}z_k\right)\cdot\left(\sum_{k\in\mathcal{K}_{\mathrm{post}}}z_k\right)^*\right\},\qquad(2)$$

where D is expressed as $D=K-L\cdot(K_p/2-1)-1$ and z_k is already pre-compensated by the prior synchronization stages. As already mentioned in the previous Section, the estimation range of (2) is limited to $|\Delta f T|<1/(2\,D)$.

Up to this point, frequency synchronization for an L-PP pilot constellation was considered. An alternative that we here consider, is the P-M-P pilot constellation suitable for long bursts, such as the MPEG2 burst. The synchronization procedure is then similar to the approach described above. Both the first and the second estimation/synchronization stage are applied separately to the pre- and postamble. However then, there is an intermediate stage, making use of the midamble by applying the FFT-based estimation [7] and, subsequently, the L&R algorithm [8] to it. The last stage (2) is again limited to only the pilot symbols in pre- and postamble.

Data-aided phase offset estimation is performed subsequent to frequency offset estimation:

$$\hat{\vartheta}=\arg\left\{\sum_{k\in\mathcal{K}_{\mathrm{p}}}z_k\right\}.\qquad(3)$$

Note that in case of perfect frequency synchronization and a constant phase offset, the accuracy of the phase estimator is independent of the positions of the pilot symbols in the burst.

6. TURBO SYNCHRONIZATION

Turbo synchronization offers an iterative approximate solution to a maximum-likelihood (ML) estimation problem. Given the likelihood function $p(\boldsymbol{r}|\boldsymbol{b})$, with $\boldsymbol{b}=[\vartheta,\Delta f]^{\mathrm{T}}$, the ML estimate of $\boldsymbol{b}$ can be computed as:

$$\hat{\boldsymbol{b}}_{\mathrm{ML}}=\arg\max_{\tilde{\boldsymbol{b}}}\left\{\ln p(\boldsymbol{r}|\tilde{\boldsymbol{b}})\right\},\qquad(4)$$

where $\tilde{\boldsymbol{b}}$ is a trial vector of the parameter set and $p(\boldsymbol{r}|\boldsymbol{b})$ can be computed according to

$$p(\boldsymbol{r}|\boldsymbol{b})=\int_{\boldsymbol{a}}p(\boldsymbol{r}|\boldsymbol{a},\boldsymbol{b})\;p(\boldsymbol{a})\;d\boldsymbol{a}.\qquad(5)$$

The Expectation-Maximization (EM) approach [9] is a method that iteratively implements ML estimation and offers the mathematical framework for turbo synchronization [3]. Using the superscript (n) to denote the iteration index, the estimators for frequency and phase offsets are given as follows:

$$\Delta\hat{f}^{(n)}=\arg\max_{\Delta\tilde{f}}\left\{\left|\sum_{k\in\mathcal{K}}r_k\;e^{-j2\pi\Delta\tilde{f}Tk}\alpha_k^*\left(\boldsymbol{r},\hat{\boldsymbol{b}}^{(n-1)}\right)\right|\right\}\qquad(6)$$

$$\hat{\vartheta}^{(n)}=\arg\left\{\sum_{k\in\mathcal{K}}r_k\;e^{-j2\pi\Delta\hat{f}^{(n)}Tk}\alpha_k^*\left(\boldsymbol{r},\hat{\boldsymbol{b}}^{(n-1)}\right)\right\},\qquad(7)$$

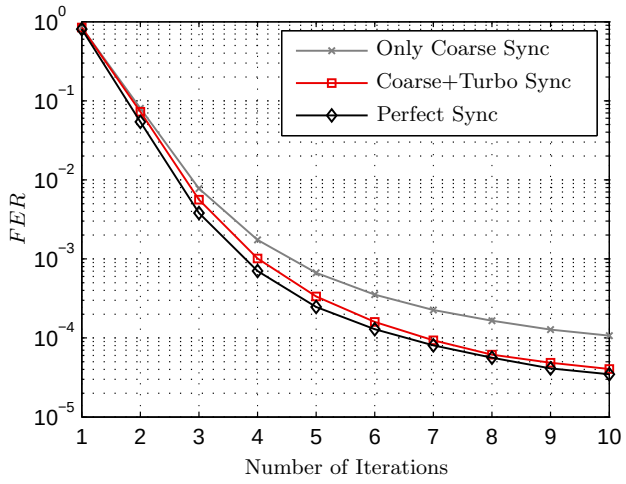

(a) ATM, $E_b/N_0 = 1.9$dB, $\eta = 0.13$.

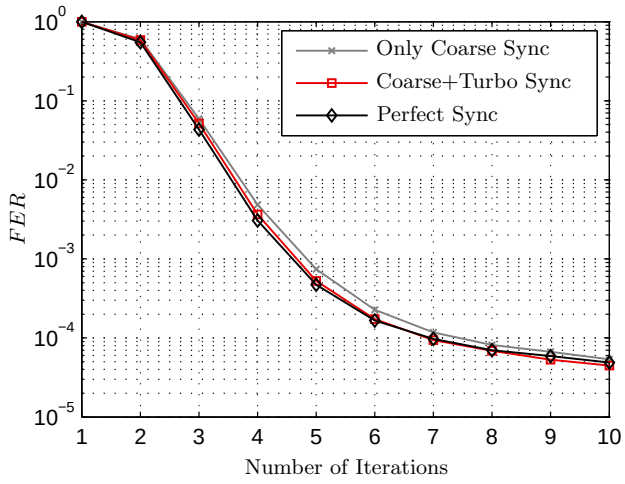

(b) MPEG2, $E_b/N_0 = 1.5$dB, $\eta = 0.08$.

Figure 4: FER vs. Iterations

where the so-called soft-symbols α_k can be calculated as

$$\alpha_k\Big(\boldsymbol{r}, \hat{\boldsymbol{b}}^{(n-1)}\Big) = \sum_{a\in\mathcal{A}} a\; P\Big(a_k = a|\boldsymbol{r}, \hat{\boldsymbol{b}}^{(n-1)}\Big). \tag{8}$$

The soft-symbols α_k depend on a-posteriori probabilities $P\big(a_k = a|\boldsymbol{r}, \hat{\boldsymbol{b}}^{(n-1)}\big)$. The soft information provided by a turbo decoder can be used for their approximation. This immediately suggests to perform synchronization and iterative soft decoding jointly in a loop.

Note that for $k \in \mathcal{K}_p$, the soft-symbols in (6) and (7) are replaced by the known transmitted symbols a_k.

6.1 Low-Complexity Estimators

Since the EM rule for frequency estimation (6) provokes a computationally expensive maximum search, a low-complexity frequency estimator based on linear regression has been introduced in [10]. The estimator subdivides the burst into M blocks and the K_m unmodulated symbols $z_k = r_k\alpha_k^*$ within each block are subsequently summed up. Due to the summation, the averaged symbols are characterized by an increased SNR. Let $\bar{k}_m$ denote the position of the average symbol of the m^{th} block and let $\bar{\varphi}_m$ denote its phase. Then, the estimator for the carrier frequency can finally be expressed as

$$\Delta\hat{f} = \frac{1}{2\pi T}\; \frac{\sum\limits_{m=1}^{M}\big(\bar{k}_m - \bar{k}\big)\big(\bar{\varphi}_m - \bar{\varphi}\big)}{\sum\limits_{m=1}^{M}\big(\bar{k}_m - \bar{k}\big)^2}. \tag{9}$$

The estimate of the constant phase ϑ can subsequently be obtained from

$$\hat{\vartheta} = \bar{\varphi} - 2\pi\Delta\hat{f}T\bar{k}. \tag{10}$$

Assuming that M is sufficiently large, it can be demonstrated by means of simulations that the EM estimator (6) and the linear regression estimator (9) show virtually the same performance in terms of estimation accuracy.

7. SIMULATIONS

The simulations presented in this paper show the performance for DVB–RCS traffic bursts. The regarded formats are ATM and MPEG2. The data is encoded with a parallel concatenated turbo code. Details concerning the code and the interleaver can be found in the standard [1]. Here, we just consider the code rate $r = 1/3$. The ratio of pilot symbols is $\eta = 0.13$ for the ATM burst and $\eta = 0.08$ for the MPEG2 burst, respectively. These values were chosen based on the results provided in the appendix and an additional margin. The pilot constellation of the ATM burst is as in Fig. 2(b) with $L = 6$. The MPEG2 burst has a P-M-P pilot constellation, where pre- and postamble consist of $1/4\,K_p$ each. The residual half of the pilot symbols establishes the equally distributed midamble. Similar optimization steps can be provided for other bursts and other code rates.

Fig. 4 shows the convergence in terms of the frame error rate (FER) versus the number of iterations. The curves from top to bottom correspond to the situation with only coarse synchronization (cross markers), with coarse and turbo synchronization (square markers) and without any synchronization error (diamond markers). It is obvious that turbo synchronization is especially valuable for the ATM burst. It can save up to two MAP decoder iterations. As the complexity of one turbo synchronization iteration is negligible in comparison to a MAP decoder iteration, this is a reasonable approach to save receiver complexity, i.e. to save iterations. Regarding the energy consumption in the transmitter, turbo synchronization enables a given frame error rate at reduced E_b/N_0. Due to space limitations, this result is not presented here. However, the gain is with about 0.1dB rather marginal.

Fig. 4(b) illustrates that MPEG2 bursts do not really profit from turbo synchronization. As this burst consists of significantly more symbols than the ATM burst, two important criteria for the coarse synchronization are fulfilled: firstly, the total amount of energy carried by the pilot symbols is high enough for the coarse synchronization to achieve its theoretical optimum and, secondly, the distance D between pre- and postamble is so large, that the theoretical optimum of the coarse estimation unit already enables a sufficiently accurate synchronization. Based on the results presented in the appendix, it can be shown that for a P-M-P pilot constellation, $\eta > 0.05$ must be met for the MPEG2 burst. Thus, in this context, turbo synchronization is not really an option to save bandwidth either.

8. CONCLUSION

In this paper, we consider frequency and phase offset synchronization issues for the DVB–RCS standard. The positioning of the pilot symbols as well as their amount is theoretically motivated and optimized. Furthermore, we examine to what extend turbo synchronization is a valuable ap-

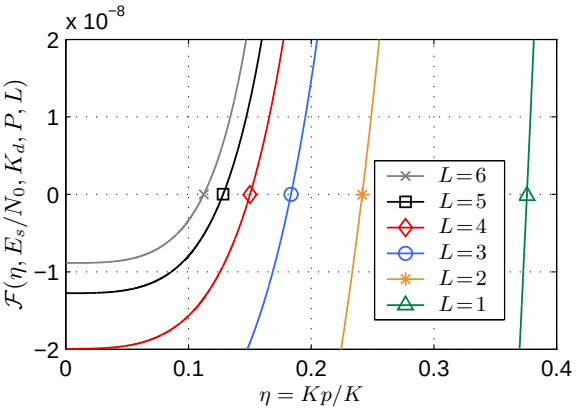

Figure 5: ATM, $E_b/N_0 = 2.2$dB, $r = 1/3$, $P = 10^{-9}$.

proach to save transmit energy and receiver complexity. It is shown, that turbo synchronization can significantly reduce the receiver complexity for the ATM burst, but has rather negligible advantages for the MPEG2 burst.

A. APPENDIX

The appendix exemplarily presents the lower limit for η in the case of an L-PP pilot constellation (Fig. 2(b)).

The lower bound for the estimation error variance that can be obtained from an L-spaced preamble, or an L-spaced postamble, respectively, each consisting of $K_p/2$ pilot symbols is given as [6]:

$$CRB_{\Delta fT} = \frac{3}{2\pi^2 \frac{E_s}{N_0} L^2 K_p/2 (K_p/2-1)^2} \approx \frac{12}{\pi^2 \frac{E_s}{N_0} L^2 K_d^3 (\frac{\eta}{1-\eta})^3} \quad (11)$$

Given that an estimator exists that achieves the CRB (11) for both pre- and postamble, the lower bound for the MSE of the linear combination of these estimates ($\Delta\hat{f}^{(1)} = 1/2 \cdot (\Delta\hat{f}_{\text{pre}} + \Delta\hat{f}_{\text{post}})$) is then given as:

$$\sigma^2 = \mathrm{E}\left\{(\Delta f - \Delta\hat{f}^{(1)})^2 T^2\right\} = \frac{6}{\pi^2 \frac{E_s}{N_0} L^2 K_d^3 (\frac{\eta}{1-\eta})^3}. \quad (12)$$

In order to profit from the distance D between pre- and postamble, we introduced the last frequency estimation stage (2). As already mentioned, the estimation range is then limited to $|\Delta fT| < 1/(2D)$. Assuming a normally distributed residual error, we get the condition

$$2 \int_{1/(2D)}^{\infty} \frac{1}{\sqrt{2\pi\sigma^2}} e^{-\frac{x^2}{2\sigma^2}} dx < P \quad (13)$$

with P being the probability that the last frequency estimation stage produces an estimate that has either the wrong sign or differs from the actual value by a multiple of 2π. Making use of the definition

$$\mathrm{erfc}(x) = \frac{2}{\sqrt{\pi}} \int_x^{\infty} e^{-t^2} dt$$

then yields

$$\sigma^2 = \frac{6}{\pi^2 \frac{E_s}{N_0} L^2 K_d^3 (\frac{\eta}{1-\eta})^3} < \left[\frac{1/(2D)}{\mathrm{erfc}^{-1}(P)\sqrt{2}}\right]^2. \quad (14)$$

In order to determine the minimum η, we rewrite (14), insert $D = K - L \cdot (K_p/2 - 1) - 1$ and define a function $\mathcal{F}$:

$$\mathcal{F}(\eta, E_s/N_0, K_d, L, P) := \frac{\eta^3}{(1-\eta)[K_d(1 - L/2 \cdot \eta) + (L-1)(1-\eta)]^2} - \frac{48[\mathrm{erfc}^{-1}(P)]^2}{\pi^2 E_s/N_0 L^2 K_d^3} > 0. \quad (15)$$

For the ATM burst, we choose the upper limit of $L = 6$ and the target E_s/N_0 for a frame error rate of $FER = 10^{-5}$ taken from [11]. As a cycle slip should have a probability of occurrence of at least a few orders of magnitude smaller than the decision error probability for perfect synchronization [2], we choose $P = 10^{-9}$. The minimum η that is then feasible, is the point where $\mathcal{F}$ crosses zero: here $\eta > 0.11$ (Fig. 5). The curves for the MPEG2 burst have a similar shape. However, due to the increased number of K_p, they are slightly shifted to the left.

REFERENCES

[1] ETSI, "Digital Video Broadcasting (DVB); Interaction Channel for Satellite Distribution Systems; (EN 301 790 V1.4.1)," Sept. 2005.

[2] H. Meyr, M. Moeneclaey, S. Fechtel, *Digital Communication Receivers: Synchronization, Channel Estimation and Signal Processing*, 1st ed. New York, NY: John Wiley & Sons, 1998.

[3] N. Noels, V. Lottici, A. Dejonghe, H. Steendam, M. Moeneclaey, M. Luise, L. Vandendorpe, "A Theoretical Framework for Soft-Information-Based Synchronization in Iterative (Turbo) Receivers," *EURASIP Journal on Wireless Communications and Networking, Special Issue on Advanced Signal Processing Algorithms for Wireless Communications*, vol. 2005, no. 2, pp. 117–129, April 2005.

[4] V. Lottici, M. Luise, "Embedding Carrier Phase Recovery Into Iterative Decoding of Turbo-Coded Linear Modulations," *IEEE Transactions on Communications*, vol. 52, no. 4, pp. 661–669, Apr. 2004.

[5] H. Wymeersch, M. Moeneclaey, "Iterative Code-Aided ML Phase Estimation and Phase Ambiguity Resolution," *Eurasip Journal on Applied Signal Processing. Special Issue on Turbo Processing*, vol. 2005, no. 6, pp. 981–988, May 2005.

[6] J.A. Gansman, J.V. Krogmeier, M.P. Fitz, "Single Frequency Estimation with Non-Uniform Sampling," in *Proc. of 30th Asilomar Conference on Signals, Systems and Computers*, vol. 1, Pacific Grove, California, USA, Nov. 1996, pp. 399–403.

[7] L. C. Palmer, "Coarse Frequency Estimation Using the Discrete Fourier Transform," *IEEE Transactions on Information Theory*, vol. 20, no. 1, pp. 104–109, Jan. 1974.

[8] M. Luise, R. Reggiannini, "Carrier Frequency Recovery in All-Digital Modems for Burst-Mode Transmissions," *IEEE Transactions on Communications*, vol. 43, no. 2/3/4, pp. 1169–1178, Feb.-Apr. 1995.

[9] A. P. Dempster, N. M. Laird, D.B. Rubin, "Maximum-Likelihood from Incomplete Data via the EM Algorithm," *Journal of the Royal Statistical Society, Series B*, vol. 39, no. 1, pp. 1–38, Jan. 1977.

[10] S. Godtmann, A. Pollok, N. Hadaschik, W. Steinert, G. Ascheid, H. Meyr, "Joint Iterative Synchronization and Decoding Assisted by Pilot Symbols," *Proc. of IST Mobile & Wireless Communication Summit*, June 2006.

[11] ETSI, "Digital Video Broadcasting (DVB); Interaction Channel for Satellite Distribution Systems; Guidelines for the use of EN 301 790; (TR 101 790 V1.2.1)," Jan. 2003.